Multiarrangement photodissociation calculations utilizing negative imaginary potentials

Cite as: J. Chem. Phys. **114**, 54 (2001); https://doi.org/10.1063/1.1329642
Submitted: 06 July 2000 • Accepted: 10 October 2000 • Published Online: 19 December 2000

Dmitri G. Abrashkevich, Paul Brumer and Moshe Shapiro

Multiarrangement photodissociation calculations utilizing negative imaginary potentials

Dmitri G. Abrashkevich and Paul Brumer
Chemical Physics Theory Group, Department of Chemistry and Photonics Research Ontario, University of Toronto, Toronto M5S 3H6, Canada

Moshe Shapiro
Chemical Physics Department, The Weizmann Institute of Science, Rehovot 76100, Israel

(Received 6 July 2000; accepted 10 October 2000)

A new method for calculating total and partial cross sections for photodissociation processes which produce more than one chemical product is presented. By using negative imaginary absorbing potentials, the method reduces the multiarrangement problem to a set of single-arrangement problems. In this way, the state-to-state photodissociation transition amplitudes are calculated directly using the artificial channel method coupled to an efficient log–derivative propagator. In addition, the discrete position operator representation is used to significantly simplify the calculations of the potential matrix elements. The method is shown to provide accurate cross sections for the resonant photodissociation of a model CO_2 system. © *2001 American Institute of Physics.* [DOI: 10.1063/1.1329642]

I. INTRODUCTION

Branching, or multiarrangement, photodissociation, leading to a number of chemically distinct products, is the subject of many theoretical and experimental studies. Recently, interest has turned to controlling the ratio of products of such a photodissociation process. This goal can be achieved using quantum interference phenomena, via the methods of coherent and optimal control.[1–8]

Continued progress towards this goal demands the development of effective theoretical tools for treating multiarrangement photodissociation reactions. Multiarrangement photodissociation is in essence a reactive scattering process which occurs on an excited potential surface, accessed from a bound state of the ground electronic state. As such, it is subject to many of the computational difficulties associated with multiarrangement problems, the main one being the need to simultaneously solve the Schrödinger equation in all the product arrangements. This heavy computational burden grows roughly as the third power of the number of arrangements. In spite of these difficulties, significant progress has been made in the past few decades via the development of efficient theoretical methods for treating the multiarrangement reactive scattering problem. In particular, various collinear[9] and three-dimensional[10] reactive scattering systems have been treated using both the time-dependent and time-independent versions of the negative imaginary absorbing potential (NIAP) method. In this article we make use of this approach to develop a method of computing photodissociation amplitudes for multiarrangement photodissociation problems.

The negative imaginary potential approach is of special interest since it enables one to convert a multiarrangement problem in real arithmetic into a set of (complex arithmetic) single-arrangement problems. In this way the numerical effort grows, in principle, linearly with the number of product arrangements, a significant reduction by comparison with the third power law noted above. However, this reduction in computational effort is usually accompanied by a loss of information. In particular, in the NIAP approach to reactive scattering one introduces absorbing potentials in order to capture all the flux entering the products' region. The negative imaginary potential is introduced at the entrance to the products' configuration subspace, while not affecting the wave function in the reactants subspace.[9] When this is achieved, the resulting nonunitarity in the *S*-matrix of the reactants subspace reflects exactly the flux arriving at the products' channels. In this way the (reactants)-state-to-all-(products)-states reactive *flux* can be estimated.

In this study we show how in the context of the artificial channel method (ACM)[11] it is possible to use the NIAP method to calculate *state-to-state* photodissociation amplitudes. NIAP method allows the direct calculation of the detailed state-to-state *amplitudes*[12] because in photodissociation the initial state is a bound state of the combined system which belongs to neither products. With the NIAP method, it is therefore possible to separately calculate transitions from the initial state to any of the final states of any chemical product.

Photodissociation calculations necessitate the calculation of dipole matrix elements from an initial bound state to a final scattering state describing the reactive scattering process. This task can be done very efficiently using the ACM,[11] which allows for the direct evaluation of the state-to-state transition amplitudes, without the explicit generation of the bound or the continuum wave functions. The ACM has been used extensively in the past and shown to be highly accurate for single arrangement photodissociation calculations.[13] It is therefore eminently suitable, as shown below, for applications of the NIAP method.

Additional features of the methodology introduced here

are the coupling of the efficient log–derivative propagator to the ACM[14] and the use of the discrete position operator representation (DPOR)[15] to evaluate the potential matrix elements. This representation, which falls under the class of discrete variable representations (DVR),[16] allows for an optimal choice of ''quadrature'' points, which are tailored specifically to the type of target and number of channels under consideration, thus simplifying and speeding up the calculations.

An alternative approach would be to employ wave packet propagation techniques.[17] However, wave packet computations with realistic pulses [rather than the ultrashort $\delta(t-t')$ pulse commonly used], necessitate repeating the entire computation for each new set of photolysis laser parameters. In contrast, in the ACM and other time-independent methods, whenever the photolysis laser can be treated by first-order perturbation theory, one needs to produce the photodissociation amplitudes at each energy only once. The results can then be convoluted for any laser pulse configuration with only minor additional computational effort.[18]

The theory and its implementation are described below (Sec. II). Applications, provided in Sec. III, are here restricted for simplicity to a collinear model, that of the multiarrangement photodissociation of CO_2. This model, which has been extensively studied in the past,[19–24] possesses a rather complicated spectrum, composed of a rich resonant structure superimposed on a smooth background continuum. It thus provides a stringent test of the NIAP method. We note that there are no fundamental limitations which prevent applying this procedure to three-dimensional multiarrangement problems.

II. METHOD

Consider a polyatomic molecule initially in a vibrational state of the ground electronic state, of total energy E_i, undergoing a transition to an electronically excited state by absorbing a photon of frequency ω. For simplicity, we consider the collinear triatomic molecule ABC with two possible different product arrangements:

$$\mathrm{B+AC}\leftarrow\mathrm{ABC}+\hbar\omega\rightarrow\mathrm{A+BC}.$$

The state-to-state photodissociation cross sections $\sigma_{f,i}(E)$ can be written as

$$\sigma_{fi}(E)=\frac{4\pi\omega}{c}|A_{f,i}(E)|^2, \tag{1}$$

where E is the total energy after photon absorption ($E=E_i+\hbar\omega$), and $A_{f,i}(E)$ are the photodissociation amplitudes, given as

$$A_{f,i}(E)=\langle\Psi_E^{-(f)}|d|\Psi^{(i)}\rangle. \tag{2}$$

Here the $-(f)$ superscript represents a scattering solution with outgoing flux in the fth channel, and the (i) superscript denotes the ith bound state. The symbol d stands for the projection of the transition-dipole along the polarization vector of the photon.

When the multiarrangement problem under consideration is reduced to a set of single-arrangement problems, as described below, one treats the final arrangement channel of interest using its appropriate Jacobi coordinates and reduced masses. Thus for the $\mathrm{ABC}+\hbar\omega\rightarrow\mathrm{A+BC}$ channel, we use the A+BC variables, etc.

The Schrödinger equations describing the three-body collinear system in the ground and excited states, expressed in (R,r)—the A+BC Jacobi coordinates, are,

$$\left[-\frac{\hbar^2}{2\mu}\frac{\partial^2}{\partial R^2}-\frac{\hbar^2}{2m}\frac{\partial^2}{\partial r^2}+W_g(R,r)-E_i\right]\Psi^{(i)}(R,r)=0, \tag{3}$$

$$\left[-\frac{\hbar^2}{2\mu}\frac{\partial^2}{\partial R^2}-\frac{\hbar^2}{2m}\frac{\partial^2}{\partial r^2}+W_e(R,r)-E\right]\Psi_E^{-(f)}(R,r)=0, \tag{4}$$

where $W_g(R,r)$ and $W_e(R,r)$ are the ground and excited state potentials, μ is the A−BC reduced mass, $\mu=M_\mathrm{A}(M_\mathrm{B}+M_\mathrm{C})/(M_\mathrm{A}+M_\mathrm{B}+M_\mathrm{C})$, and $m=M_\mathrm{B}M_\mathrm{C}/(M_\mathrm{B}+M_\mathrm{C})$ is the reduced mass of the product diatom of interest.

In order to solve the two-dimensional Schrödinger equations, in both ground [Eq. (3)] and excited [Eq. (4)] manifolds, the total wave function $\Psi^{(i)}(R,r)$ or $\Psi_E^{-(f)}(R,r)$, is expanded in a basis set of the product diatomic vibrational states, $\{\phi_n^s(r)\}$, $s=g(\mathrm{ground}),\ e(\mathrm{excited})$,

$$\begin{aligned}\Psi^{(i)}(R,r)&=\sum_{n=1}^{N_g}\phi_n^g(r)F_n^{(i)}(R),\\ \Psi_E^{-(f)}(R,r)&=\sum_{n=1}^{N_e}\phi_n^e(r)F_n^{-(f)}(R).\end{aligned} \tag{5}$$

The number of channels (N_g or N_e) appropriate to each state is taken sufficiently large to ensure convergence of the expansions.

Given the above expansion, the photodissociation amplitudes [Eq. (2)] are given as

$$A_{f,i}(E)=\langle\mathbf{F}^{-(f)}|\cdot\mathsf{d}_{e,g}\cdot|\mathbf{F}^{(i)}\rangle, \tag{6}$$

where $|\mathbf{F}\rangle$ represents a column of ket vectors and $\langle\mathbf{F}|$ represents a row of bra vectors. The symbol $\mathsf{d}_{e,g}$ denotes a rectangular $(N_e\times N_g)$ matrix.

The functions $\{\phi_n^s(r)\}$ are the orthonormal set of solutions of the

$$h_s(r)\phi_n^s(r)=\epsilon_n^s\phi_n^s(r),\quad s=g,e, \tag{7}$$

product diatomic Schrödinger equations in the ground or excited states. ϵ_n^s are the product diatomic vibrational eigenvalues and $h_s(r)$ are the product diatomic vibrational Hamiltonians in the ground or excited electronic states,

$$h_s(r)=-\frac{\hbar^2}{2m}\frac{d^2}{dr^2}+v_s(r), \tag{8}$$

where $v_s(r)=\lim_{R\rightarrow\infty}W_s(R,r)$ is the asymptotic diatomic potential.

Taking the scalar product of Eqs. (3) and (4) with the $\{\langle\phi_n^s(r)|\}$ states, leads to the well-known coupled-channels system of equations for the $F_n^{(s)}(R)$ expansion coefficients, which can be written in compact matrix notation as

$$\left[\left(-\frac{\hbar^2}{2\mu}\frac{d^2}{dR^2}-E\right)\mathsf{I}+\boldsymbol{\epsilon}^s+\mathsf{V}^s\right]\mathsf{F}^{(s)}(R)=0, \tag{9}$$

where $\mathsf{F}^{(s)}$ is the matrix of solutions and I is the unity matrix, both of dimension $N_s\times N_s$. The matrices $\boldsymbol{\epsilon}^s$ and V^s are defined as

$$\epsilon^s_{n,m}=\epsilon^s_n\delta_{n,m} \tag{10}$$

and

$$\mathsf{V}^s_{n,m}(R)=\int dr\ \phi^{*s}_n(r)V^s(R,r)\phi^s_m(r). \tag{11}$$

Here $V^s(R,r)$ is the interaction potential defined as

$$V^s(R,r)=W_s(R,r)-v_s(r). \tag{12}$$

We now reduce these equations to a set of single arrangement equations. To do so, we modify $V^s(R,r)$ by placing short-range NIAPs, $U_I(R,r)$, well into the entrance region of all the products, save for the product of interest. A perfectly absorbing potential, if placed sufficiently far into the products region, will not significantly affect the wave function in the region of the product of interest. When the ''perfect absorbance'' condition is met, the photodissociation amplitude to the product of interest will include the loss of flux due to transitions to all other products. By repeating the calculations for different products of interest we can thus extract all the state-to-state photodissociation amplitudes.

Various forms of absorbing potential can be used. The convenient form adopted here is the linear ramp:[10]

$$U_I(R,r)=\begin{cases}-iU_{I0}\dfrac{r-r_{1I}}{r_{2I}-r_{1I}}, & r_{1I}\leqslant r\leqslant r_{2I},\\ 0, \quad \text{otherwise},\end{cases} \tag{13}$$

where $0\leqslant R\leqslant\infty$. The constant U_{I0} must fulfill the following two conditions:[10]

$$\hbar E_t^{1/2}/(\Delta r_I\sqrt{8\mu})\ll U_{I0}\ll\Delta r_I\sqrt{8\mu}E_t^{3/2}/\hbar, \tag{14}$$

where, E_t is the translational energy in the product of interest arrangement, μ is the reduced mass in that arrangement, and $\Delta r_I=r_{2I}-r_{1I}$. The left-hand inequality [Eq. (14)] guarantees that all the flux entering into this potential region is absorbed, and the right-hand one guarantees that there is no reflection off the imaginary potential.

The V^e matrix [Eq. (11)] is now replaced by a matrix, denoted $\tilde{\mathsf{V}}^e$, derived from the

$$\tilde{V}^e(R,r)=W_e(R,r)+U_I(R,r)-v_e(r) \tag{15}$$

potential.

With $\tilde{\mathsf{V}}^e$ matrix replacing V^e, we now utilize Eq. (9) to obtain the photodissociation amplitudes. To do so we utilize the ACM, wherein one solves a combined set of coupled-channels equations for the bound and continuum manifolds.[11] To account for the different boundary conditions of the bound and continuum parts, one introduced an additional ''artificial'' channel (identified by subscripts a), serving as a source term for the bound manifold. The resultant set of equations can be written as

$$\left(-\frac{\hbar^2}{2\mu}\frac{d^2}{dR^2}+\epsilon^e_n-E\right)F^{(f)}_n(R)+\sum_{n'}\tilde{V}^e_{n,n'}(R)F^{(f)}_{n'}(R)$$
$$=-\sum_{m'}d_{n,m'}(R)F^{(i)}_{m'}(R), \tag{16}$$

$$\left(-\frac{\hbar^2}{2\mu}\frac{d^2}{dR^2}+\epsilon^g_m-E\right)F^{(i)}_m(R)+\sum_{m'}V^g_{m,m'}(R)F^{(i)}_{m'}(R)$$
$$=-V^a_m(R)F_a(R), \tag{17}$$

$$\left(-\frac{\hbar^2}{2\mu}\frac{d^2}{dR^2}-E+\epsilon_a+V_a(R)\right)F_a(R)=0, \tag{18}$$

where the dipole matrix, $d_{m,n}(R)$, is given by

$$d_{m,n}=\int dr\ \phi^{*e}_m(r)d_{e,g}\phi^g_n(r). \tag{19}$$

Equation (16) describes a continuum manifold, coupled to a bound manifold of Eq. (17) which, in turn, is coupled to the artificial channel introduced in Eq. (18). The artificial channel, serving as a source term, is governed by the ϵ_a asymptotic energy, the V_a potential, and the choice of V^a_n coupling potentials. The $\tilde{V}^e_{n,m}(R)$ and $V^g_{n,m}(R)$ matrices are given by matrix elements of Eqs. (12) and (15). In the Franck–Condon approximation used here, these matrix elements are given as

$$d_{m,n}=\overline{d}_{e,g}\int dr\ \phi^{*e}_m(r)\phi^g_n(r). \tag{20}$$

Although the combined set of equations is now somewhat larger than the separate set of scattering equations of Eq. (9), the difference is not too large because the number of additional equations due to the bound part is usually small. This is more than compensated for by obviating the need to calculate wave functions.

Equations (16)–(18) can be written in a more compact form using matrix notation

$$\left\{\left(-\frac{\hbar^2}{2\mu}\frac{d^2}{dR^2}+\boldsymbol{\epsilon}-E\right)\mathsf{I}+\mathsf{V}(R)\right\}\mathsf{F}(R)=0, \tag{21}$$

where the potential matrix is of the form

$$\mathsf{V}(R)=\begin{pmatrix}V_a(R) & \mathbf{O}^\dagger & \mathbf{O}^\dagger\\ \mathbf{O} & \tilde{\mathsf{V}}^e(R) & d_{e,g}(R)\\ \mathbf{V}^a(R) & \mathsf{O} & \mathbf{V}^g(R)\end{pmatrix}, \tag{22}$$

with $\boldsymbol{\epsilon}$ given by

$$\boldsymbol{\epsilon}=\begin{pmatrix}\epsilon_a & \mathbf{O}^\dagger & \mathbf{O}^\dagger\\ \mathbf{O} & \boldsymbol{\epsilon}^e & \mathsf{O}\\ \mathbf{O} & \mathsf{O} & \boldsymbol{\epsilon}^g\end{pmatrix}. \tag{23}$$

Here, A represents a rectangular matrix, $\mathbf{A}$ represents a column vector, and the † symbol denotes the Hermitian adjoint (the complex-conjugate transpose).

The S-matrix derived from Eq. (21) can be obtained using a variety of multichannel propagation schemes.[25] Of greatest interest to us are the elements of the S-matrix which

connect the artificial channel to the continuum subspace. These matrix elements can be written, using standard expressions, as

$$S_{f,a}(E)=2\pi i\langle \mathbf{F}^{-(f)}|\cdot \mathsf{d}_{e,g}\cdot|\mathbf{F}^{+(a)}(E)\rangle. \tag{24}$$

Here, an $|\mathbf{A}\rangle$ symbol represents a column of ket vectors and an $\langle\mathbf{A}|$ symbol represents a row of bra vectors. The $\pm(j)$ superscript represents a scattering solution with an incoming/outgoing flux in the jth channel.

It can be shown[11,14] that with the special nonsymmetric form of Eq. (21) the above matrix elements become

$$S_{f,a}(E)=2\pi i \times\sum_i \frac{\langle \mathbf{F}^{-(f)}|\cdot \mathsf{d}_{e,g}\cdot|\mathbf{F}^{(i)}\rangle\langle \mathbf{F}^{(i)}|\cdot \mathbf{V}^a|F_a^{+(a)}(E)\rangle}{E-E_i}. \tag{25}$$

It follows from Eq. (25) that all the elements belonging to the $S_{f,a}$ column have poles at E_i, the bound state energies of the system, and that the residues of these poles are directly related to the desired photodissociation amplitudes of Eq. (6),

$$A_{f,i}(E)=\langle \mathbf{F}^{-(f)}|\cdot \mathsf{d}_{e,g}\cdot|\mathbf{F}^{(i)}\rangle=\frac{1}{2\pi i}\mathrm{Res}_i\left\{\frac{S_{f,a}(E)}{a_i(E)}\right\}, \tag{26}$$

where Res_i is the ith residue, and

$$a_i(E)=\langle \mathbf{F}^{(i)}|\cdot \mathbf{V}^a|F_a^{+(a)}(E)\rangle. \tag{27}$$

The pole energies E_i and the a_i coefficients are calculated separately by replacing all the channels belonging to the excited electronic state by a single additional artificial channel a'. Channel a' is identical in form to channel a, namely we choose $\epsilon_{a'}=\epsilon_a$, $\mathbf{V}^{a'}=\mathbf{V}^{a\dagger}$, and $V_{a'}=V_a$. The $S_{a',a}$ matrix element resulting from this truncated set of equations, which is identical in structure to Eq. (21), is of the form

$$S_{a',a}(E)=2\pi i\sum_i \frac{\langle F_{a'}^{-(a')}(E)|\mathbf{V}^{a'}\cdot|\mathbf{F}^{(i)}\rangle\langle \mathbf{F}^{(i)}|\cdot \mathbf{V}^a|F_a^{+(a)}(E)\rangle}{E-E_i}=2\pi i\exp(2i\delta_a)\sum_i |a_i(E)|^2/(E-E_i). \tag{28}$$

Hence $|a_i(E_i)|^2$ are obtained as

$$|a_i(E_i)|^2=\left|\frac{1}{2\pi}\mathrm{Res}_i\, S_{a',a}(E)\right|, \tag{29}$$

and E_i are obtained as the corresponding poles positions. These poles can be located very efficiently[26] using only a few iterations (see Appendix A of Ref. 26).

Once $a_i(E_i)$ and E_i are known, the desired bound-free matrix elements are computed directly from Eq. (25). A simple shift of $E-E_i$ in the definition of the ϵ_a asymptotic energy guarantees that it suffices to solve Eq. (29) only once, i.e., that the value of $a_i(E_i)$ may be used for all energies.[11]

The above procedure guarantees[11] that the results for the final bound-free matrix elements are insensitive to the exact form of $V_a(R)$ and $V_n^a(R)$. The only limitation on the choice of $V_a(R)$ and $V_n^a(R)$ is imposed by the requirement that the artificial wave function F^a overlaps well with the bound wave functions. In the present application we have chosen V_a to be of the form, $V_a(R)=V_0\exp(-aR)$, with the value of a fixed so as to guarantee a good overlap with the bound manifold.

The calculations are then repeated in a similar fashion for each of the products of interest by placing the negative imaginary potential at the entrance to other products.

The numerical method used by us to solve Eq. (21) and to obtain the $S_{f,a}(E)$ matrix elements is the log–derivative propagation method.[25] The method converges rapidly and eliminates instability problems which can arise when the integration is started deep inside the classically forbidden region.[25,27]

In addition, in order to speed up the computations we have used the DPOR[15] to calculate the potential matrix elements. According to this method, the matrix elements $V_{n,m}(R)$ are calculated using a quadrature of the form

$$\begin{aligned} V^g_{m,m'}(R)&=\sum_{j=1}^{N_g} C^g_{m,j}V^g(R,r^g_j)C^g_{m',j}, \quad m,m'=1,\ldots,N_g,\\ \tilde{V}^e_{n,n'}(R)&=\sum_{j=1}^{N_e} C^e_{n,j}\tilde{V}^e(R,r^e_j)C^e_{n',j}, \quad n,n'=1,\ldots,N_e, \end{aligned} \tag{30}$$

where $C^s_{n,i}$, $s=g,e$, are the eigenvectors, r^s_j being the eigenvalues, of the position operator matrix, r,

$$\mathsf{r}^{(s)}_{n,m}=\int_{-\infty}^{\infty} dr\ \phi^{*s}_n(r)r\phi^s_m(r), \quad s=g,e. \tag{31}$$

If the basis is complete, $C^s_{n,i}$ also diagonalizes the potential matrix $\mathsf{V}(R,r)$, since the potential matrix can be written[15] as a function of the r matrix, $V(R,\mathsf{r})$. This is the justification for Eqs. (30). With the points and weights chosen in this way, even a small number of quadrature points can give highly accurate evaluation of the potential matrix.[15]

III. THE $CO_2\rightarrow CO+O$ PHOTODISSOCIATION

To test the utility and efficiency of this method we have examined the photodissociation of the well-studied[19,20,22–24] case of collinear CO_2 photodissociation, where the photodissociation branches to two identical products,

$$OC+O\leftarrow OCO\rightarrow CO+O.$$

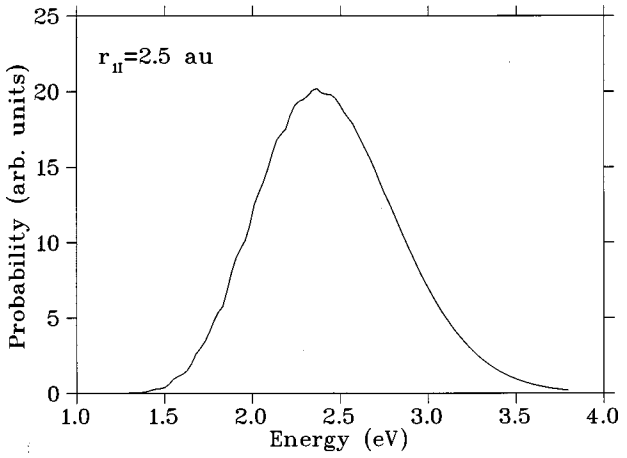

FIG. 1. The CO_2 absorption spectrum with $r_{1I}=2.5$ a.u.

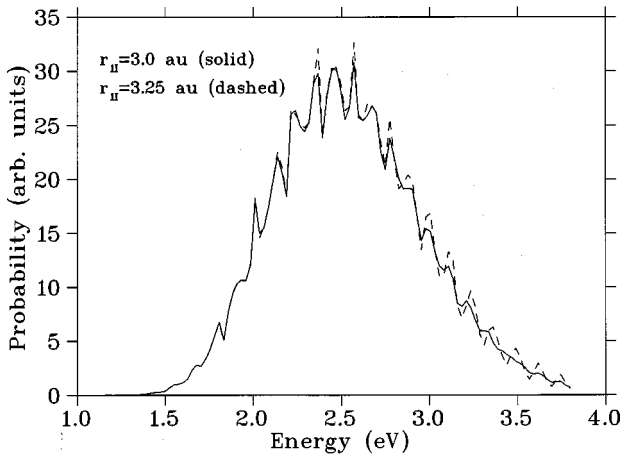

FIG. 2. The CO_2 absorption spectra obtained with $r_{1I}=3.0$ a.u. (solid line) and $r_{1I}=3.25$ a.u. (dashed line).

At the vacuum ultraviolet (VUV) photon energies of interest, the absorption spectrum consists of a sequence of resonances superimposed on a smooth continuum. From a semiclassical perspective, these structures reflect to underlying unstable periodic orbits on the excited electronic surface.[28] The large background is due to the dominant direct dissociation. We compute photodissociation into one product channel, the total photodissociation probability being twice that obtained for one channel.

In this case the $W_e(R,r)$ [Eq. (4)] is given by the Kulander–Light LEPS potential surface,[19] a surface which has a saddle point at $r_{CO}=2.41$ a.u., which is somewhat displaced from the ground state equilibrium position of 2.2 a.u. The ground state surface was composed of Morse functions in both bond-stretching coordinates r_{CO} and r_{OC}:[29,30]

$$W_g(R,r)\equiv W_g(r_{CO},r_{OC}) = v^{\text{Morse}}(r_{CO})+v^{\text{Morse}}(r_{OC}). \tag{32}$$

Here,

$$v^{\text{Morse}}(r)=D_e\{\exp[-2\alpha(r-r_{CO}^e)] - 2\exp[-\alpha(r-r_{CO}^e)]\}, \tag{33}$$

where $\alpha=1.641a_0^{-1}$, $D_e=5.453$ eV, and $r_{CO}^e=2.2a_0$. In this case, parameters of the Morse function were fitted to the equilibrium distances and force constants for the ground PES taken from the harmonic potential of Kulander *et al.*[22] The relevant reduced masses chosen are defined as, $\mu=m_O m_{CO}/(m_C+2m_O)$ and $m=m_C m_O/(m_C+m_O)$.

We consider the transition from the ground vibrational state of CO_2 to energies ranging from 1.4 to 3.7 eV above the CO+O dissociation threshold. The eigenfunctions $\{\phi_n^s(r)\}$ of the Eq. (7) with $v(r)=\lim_{R\to\infty}W_e^{\text{LEPS}}(R,r)$ were used as a basis for both the initial and final CO_2 states. The vibrational eigenenergies and the corresponding eigenfunctions of the product diatomic potentials were obtained via the renormalized Numerov method[31] and a Simpson-type quadrature was used to obtain the Franck–Condon transition matrix [Eq. (20)]. The potential parameters U_{I0} and $\Delta r=(r_{2I}-r_{1I})$ were chosen to satisfy the inequalities, Eq. (14), that guarantee no reflected flux from the $r>r_{1I}$ region. Note that the conditions in Eq. (14) must be satisfied for all translational energies at given dissociation energy E. Note also that with increasing dissociation energy E the number of open channels increases as well and more basis wave functions have to be included in the expansion of Eq. (5) in order to achieve convergence.

The specific choice of r_{1I} was found to be quite important to the quality of the results. It was obtained by starting close to the reaction region, and *gradually* increasing r_{1I} until further *small* incremental increases did not influence the results. Sample results are shown in Figs. 1–3 for $\Delta r_I=2$ a.u., $U_{I0}=0.05$ a.u., and the fixed number of channels [Eq. (5)] $N_e=80$. When r_{1I} is too small ($r_{1I}=2.5$ a.u., shown in Fig. 1) the structure atop the broad background is almost absent. In this case the absorbing boundary interferes with the oscillatory wave packet motion that produces the diffuse structure, so that the peaks are suppressed. As r_{1I} is increased the spectra begin to display the proper diffuse vibrational structure. For example, the results for $r_{1I}=3.0$ a.u. (solid line) and $r_{1I}=3.25$ a.u. (dashed line) are presented in Fig. 2 and show the convergence of the spectra. (Note, however, that complete convergence for the chosen number of channels is still not achieved for the dissociation

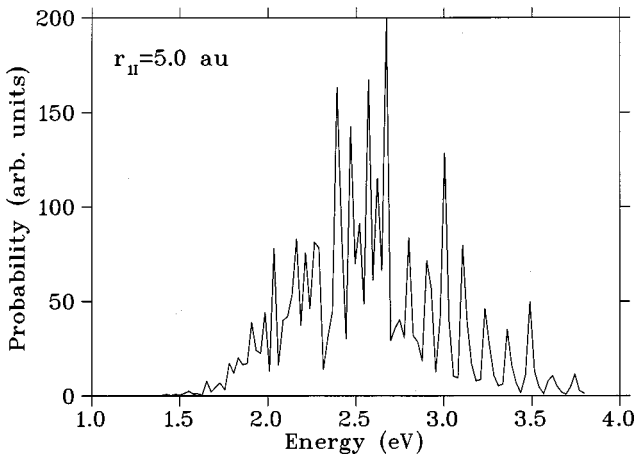

FIG. 3. The CO_2 absorption spectrum as obtained with $r_{1I}=5.0$ a.u.

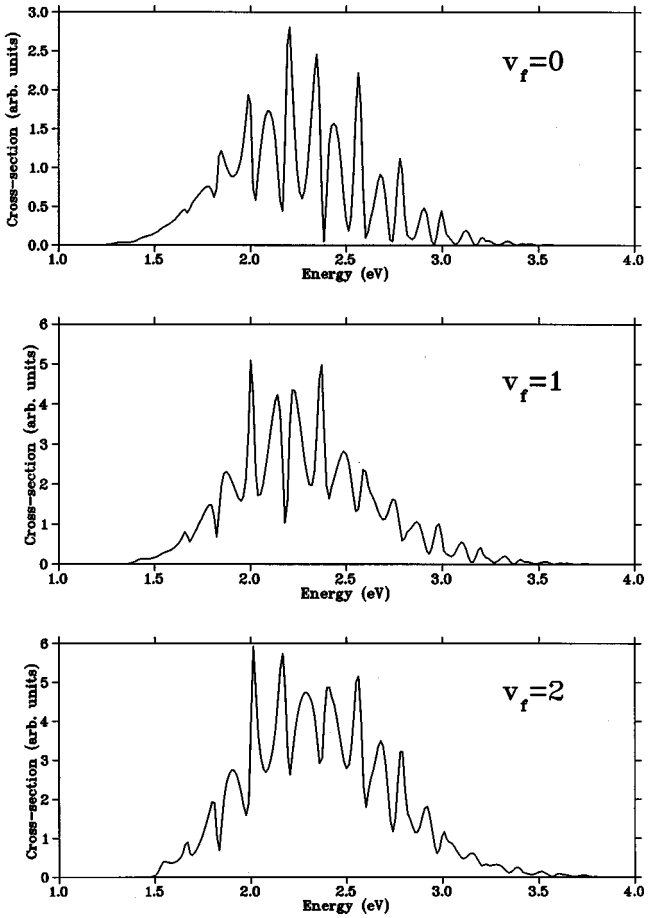

FIG. 4. Partial photodissociation probabilities excitation to the first three final vibrational quantum numbers of the CO fragment. Excitation is from the ground state of CO_2.

energies above 3 eV. In this case one would need larger values of N_e for convergence, since more channels become open as the dissociation energy increases.)

Finally, when the absorbing potential is too far from the reaction region (as Fig. 3 for $r_{1I}=5$ a.u.), we obtain nonconverged results for the number of channels used. In this case, substantially more channels would be required for convergence. Thus, choosing r_{1I} too large ($r_{1I}>4.9$ a.u.) results in a poor representation of the diffuse background, whereas choosing r_{1I} too small ($r_{1I}<3.0$ a.u.) led to poor results for the vibrational structure.

Considerations of this kind led to the best parameter choice of $r_{1I}=3.0$ a.u., $\Delta r_I=2$ a.u., and $U_{I0}=0.05$ a.u. For each r_{1I}, full convergence with respect to the number of vibrational states N_e in the basis for the excited state was reached for $E<3$ eV. The final results of our calculations of the resonant CO_2 spectrum are given by the solid line in Fig. 2. The spectrum obtained displays the series of irregular peaks, peaking at 2.36 eV, in good agreement with the results of Kulander and Light,[19] with small differences being a result of the extreme sensitivity of the results to the ground state potential.[21,23] The vibrationally resolved partial probabilities into the first three final vibrational quantum numbers ($v_f=0,1,2$) are presented in Fig. 4. Our results show that partial cross sections display the similar diffuse resonant structure as the total probabilities, and are in good agreement with previous results.[19,23]

IV. CONCLUSIONS

In this article we have introduced a new fully quantum-mechanical method of calculating photodissociation cross sections for triatomic molecules with more than one product arrangement. A short range imaginary absorbing potential has been added to the Hamiltonian operator, reducing a multiarrangement photodissociation problem to a set of single arrangement photodissociation problems. The resulting single-arrangement photodissociation is solved with the artificial channel method, utilizing an efficient log–derivative propagator. The method has been successfully applied to the photodissociation of collinear CO_2 and the diffuse vibrational structure of the CO_2 photoabsorption spectrum has been successfully reproduced in good agreement with the previous results.

This study can be readily generalized to the full three-dimensional problem. Work to that end is in progress. Applications of this method to the coherent control of collinear CH_2IBr photodissociation are the subject of a forthcoming article.[32]

ACKNOWLEDGMENT

We thank the U.S. Office of Naval Research and Photonics Research Ontario for the funding of this research.

[1] M. Shapiro and P. Brumer, Adv. At., Mol., Opt. Phys. **42**, 287 (2000); J. Chem. Soc., Faraday Trans. **93**, 1263 (1997); P. Brumer and M. Shapiro, Acc. Chem. Res. **22**, 407 (1989).
[2] S. A. Rice and M. Zhao, *Optical Control of Molecular Dynamics* (Wiley, New York, in press).
[3] W. S. Warren, H. Rabitz, and M. Dahleh, Science **259**, 1581 (1993).
[4] B. Kohler, J. L. Krause, F. Raski, K. R. Wilson, V. V. Yakovler, R. M. Whitnell, and Y. Yan, Acc. Chem. Res. **28**, 133 (1995).
[5] I. Zhu, V. Kleiman, X. Li, S.-P. Liu, K. Trentelman, and R. J. Gordon, Science **270**, 77 (1995).
[6] E. Dupont, P. B. Corkum, H. C. Liu, M. Buchanan, and Z. R. Wasilewski, Phys. Rev. Lett. **74**, 3596 (1995).
[7] A. Shnitman, I. Sofer, I. Golub, A. Yogev, M. Shapiro, Z. Chen, and P. Brumer, Phys. Rev. Lett. **76**, 2886 (1996).
[8] T. Assion, T. Baumert, M. Bergt, T. Brixner, B. Kiefer, U. Seyfried, M. Strehle, and G. Gerber, Science **282**, 919 (1998).
[9] D. Neuhauser and M. Baer, J. Phys. Chem. **90**, 4351 (1989); **91**, 4651 (1989).
[10] D. Neuhauser, R. S. Judson, R. E. Jaffe, M. Baer, and D. J. Kouri, Chem. Phys. Lett. **176**, 546 (1991).
[11] M. Shapiro, J. Chem. Phys. **56**, 2582 (1972).
[12] For NIAP calculations of state to state reactive transition probabilities see D. Neuhauser, J. Chem. Phys. **93**, 7836 (1990); D. Neuhauser, R. S. Judson, D. J. Kouri, and D. E. Adelman, Science **257**, 519 (1992); H. Szichman, M. Baer, and H. Nakamura, J. Chem. Phys. **107**, 3521 (1997).
[13] M. Shapiro, Chem. Phys. Lett. **46**, 442 (1977); E. Segev and M. Shapiro, J. Chem. Phys. **73**, 2001 (1980); **77**, 5604 (1982); S. Kanfer and M. Shapiro, J. Phys. B **16**, L655 (1983); I. Levy and M. Shapiro, J. Chem. Phys. **89**, 2900 (1988); M. Shapiro, M. J. J. Vrakking, and A. Stolow, *ibid.* **110**, 2465 (1999).
[14] M. Shapiro and R. Bersohn, Annu. Rev. Phys. Chem. **33**, 409 (1982); G. G. Balint-Kurti and M. Shapiro, Adv. Chem. Phys. **60**, 403 (1985).
[15] S. Kanfer and M. Shapiro, J. Phys. Chem. **88**, 3964 (1984).
[16] R. W. Heather and J. C. Light, J. Chem. Phys. **79**, 147 (1983).
[17] See, for example, K. C. Kulander, Phys. Rev. A **35**, 445 (1987); G. Ashkenazi, U. Banin, A. Bartana, R. Kosloff, and S. Ruhman, Adv. Chem. Phys. **100**, 229 (1997), and references therein; G. G. Balint-Kurti, R. N. Dixon, and C. C. Marston, Int. Rev. Phys. Chem. **11**, 317 (1992); H.

Flöthmann, C. Beck, R. Schinke, C. Woywod, and W. Domcke, J. Chem. Phys. **107**, 7296 (1997).
[18] M. Shapiro, J. Phys. Chem. **97**, 7396 (1993); M. Shapiro, Z. Chen, and P. Brumer, Chem. Phys. **217**, 325 (1997).
[19] K. C. Kulander and J. C. Light, J. Chem. Phys. **73**, 4337 (1980).
[20] J. P. Henshaw and D. C. Clary, J. Phys. Chem. **91**, 1580 (1987).
[21] R. Schinke and V. Engel, Chem. Phys. Lett. **124**, 504 (1986).
[22] K. C. Kulander, C. Cerjan, and A. E. Orel, J. Chem. Phys. **94**, 2571 (1991).
[23] R. Schinke and V. Engel, J. Chem. Phys. **93**, 3252 (1990).
[24] R. Sadeghi and R. T. Skodje, J. Chem. Phys. **105**, 7504 (1996).
[25] B. R. Johnson, J. Comput. Phys. **13**, 445 (1973).
[26] M. Shapiro and G. G. Balint-Kurti, J. Chem. Phys. **71**, 1461 (1978).
[27] E. B. Stechel, R. B. Walker, and J. C. Light, J. Chem. Phys. **69**, 3518 (1978).
[28] For a discussion see R. Schinke, *Photodissociation Dynamics* (Cambridge University Press, Cambridge, 1993), Chap. 8.
[29] S. Sato, J. Chem. Phys. **23**, 592 (1955); R. Weston, *ibid.* **31**, 892 (1959).
[30] M. Shapiro and R. Bersohn, J. Chem. Phys. **73**, 3810 (1980); M. Shapiro, J. Phys. Chem. **90**, 3644 (1986).
[31] B. R. Johnson, J. Chem. Phys. **67**, 4086 (1977).
[32] D. G. Abrashkevich, M. Shapiro, and P. Brumer (unpublished).